7. Green RH, Brightling CE, McKenna S, Hargadon B, Parker D, Bradding P, et al. Asthma exacerbations and sputum eosinophil counts: a randomised controlled trial. Lancet 2002;360:1715-21.
8. Normansell R, Walker S, Milan SJ, Walters EH, Nair P. Omalizumab for asthma in adults and children. Cochrane Database Syst Rev 2014;1:CD003559.
9. Hanania NA, Wenzel S, Rosen K, Hsieh HJ, Mosesova S, Choy DF, et al. Exploring the effects of omalizumab in allergic asthma: an analysis of biomarkers in the EXTRA study. Am J Respir Crit Care Med 2013;187:804-11.
10. Ducharme FM, Zemek R, Gravel J, Chalut D, Poonai N, Laberge S, et al. Determinants Of Oral corticosteroid Responsiveness in Wheezing Asthmatic Youth (DOORWAY): protocol for a prospective multicentre cohort study of children with acute moderate-to-severe asthma exacerbations. BMJ Open 2014;4:e004699.

Available online February 28, 2016.
http://dx.doi.org/10.1016/j.jaci.2015.12.1317

An inflammation-independent contraction mechanophenotype of airway smooth muscle in asthma

To the Editor:

Asthma is characterized by airway inflammation and bronchial obstruction due to airway smooth muscle (ASM) contraction. However, the underlying basis of the ASM hypercontractile state in asthma is not known. It remains equally unclear whether ASM from those with asthma has an intrinsic (genetic or epigenetic) property of increased basal tone and enhanced contractile responses.[1-5] Furthermore, current dogma suggests that any altered mechanical property of the smooth muscle, if it exists in the disease, is from airway inflammation. Here, we sought to establish, using highly quantitative methods, whether the contractile state of ASM from those with asthma has an inflammation-independent component. We applied recently developed single-cell technologies to probe the mechanical properties of isolated, passaged, primary human ASM cells.[6,7] This approach potentially avoids the interactions between airway epithelium and smooth muscle that are encountered in bronchial sections, the limited availability of fresh tissues from donors with and without asthma, and the nonspecific effects of acute dissociation of ASM cells from other tissues in biopsies. This approach may also minimize the acute effects of drugs such as β-agonists that would be expected to be administered during attempts to treat a severe asthma exacerbation. The methods used, Fourier transform traction microscopy and magnetic twisting cytometry, can be performed on the living cells adhered to matrices of varying rigidities across a pathophysiologic spectrum.

As shown in Fig 1, *A*, we used Fourier transform traction microscopy to measure ASM mechanics, with direct measurement of traction stress, and the derived net contractile moments, so as to characterize the physical properties of human ASM cells derived from donor lungs from patients with and without asthma (see Table E1 in this article's Online Repository at www.jacionline.org for subjects' demographic characteristics). For these studies, we used cells that had been passaged in standard culture media, in the absence of inflammatory mediators, and studied them under identical experimental conditions using tuned elastic matrices (ie, mimicking the physiological extremes of airway wall rigidity). Human ASM cells isolated from both sets of donor lungs showed the expected between-cell and between-donor variation in cell spreading (Fig 1, *B*) and traction (root mean square) averaged over the entire cell-projected area (Fig 1, *C*). Nested design analysis[8] revealed significant differences in both the projected area (7779 ± 303 vs 6345 ± 199 μm^2; $P = .0136$, nested ANOVA) and the average traction stress (166 ± 10 vs 119 ± 8 Pa; $P = .0316$, nested ANOVA) between those with and without asthma; there were no within-group differences. In particular, compared with ASM from those without asthma, ASM from those with asthma showed an approximately 2-fold higher (47.4 ± 4.8 vs 26.4 ± 2.4 pNm; $P = .0015$, nested ANOVA) net contractile moment, which is a scalar measure of the cell's resting contractile amplitude. These differences in physical force generation between those with and without asthma were maintained in culture with increasing passage number (Fig 1, *D*) and across the range of matrix rigidity of approximately 1 to 8 kPa (Fig 1, *E*). These results establish an unequivocal difference in resting force of cultured ASM cells between those with and without asthma, which is persistent and is apparent across a wide range of matrix rigidities mimicking that of healthy and diseased airways in the absence of the inflammatory airway milieu.

To ascertain whether ASM cells from those with asthma display increased responsiveness to locally generated spasmogens, we then measured dynamic changes in cytoskeleton stiffness in response to histamine and methacholine with magnetic twisting cytometry, as an index of single-cell contractility.[6,7] Here, RGD-coated ferrimagnetic beads are attached to ASM cell surface integrin receptors and subjected to an external magnetic field, with measurement of lateral displacement of the beads during drug exposure (see this article's Methods section in the Online Repository at www.jacionline.org). For these experiments, we used primary cells derived from 12 additional donor lungs of those with and without asthma (see Table E2 in this article's Online Repository at www.jacionline.org). On the basis of dose-response relationships (Fig E1), and experience using isolated human ASM cells, herein we chose a single dose (10 μM) of histamine or methacholine to contract the cells (Fig 2). There was heterogeneity in responses from cells of both those with and without asthma, although the latter showed greater within-group variability in the responses to both histamine (Fig 2, *A* and *C*) and methacholine (Fig 2, *B* and *D*). Using the nested effect model[8] to control for random effects from multiple cells from the same donor, and the repeated measurements, we found significant differences in the cell-stiffening response to histamine (Fig 2, *E*) and methacholine (Fig 2, *F*) between those with and without asthma. These series of studies, taken together, establish for the first time that, in the resting state, ASM from those with asthma has increased basal tone and enhanced contractility to known asthmatic spasmogens.

Almost 150 years ago, Henry Hyde Salter[9] posited that "the vice in asthma consists, not in the production of any special irritant, but in the irritability of the part irritated." Defining the asthmatic ASM mechanical phenotype, however, has been somewhat elusive.[1-5] We hypothesized that an asthmatic mechanical phenotype of ASM, if it existed, would be intrinsic to asthmatic cells, and thus allow us to study cultured ASM in the absence of inflammatory mediators, drugs used in the treatment of asthma such as corticosteroids, β-agonists, and antagonists to histamine and acetylcholine receptors, or influences from the epithelium. Our results from the present study indicate that ASM cells from those with asthma have increased cell traction forces at baseline, and enhanced stiffening (contraction) in response to activation of

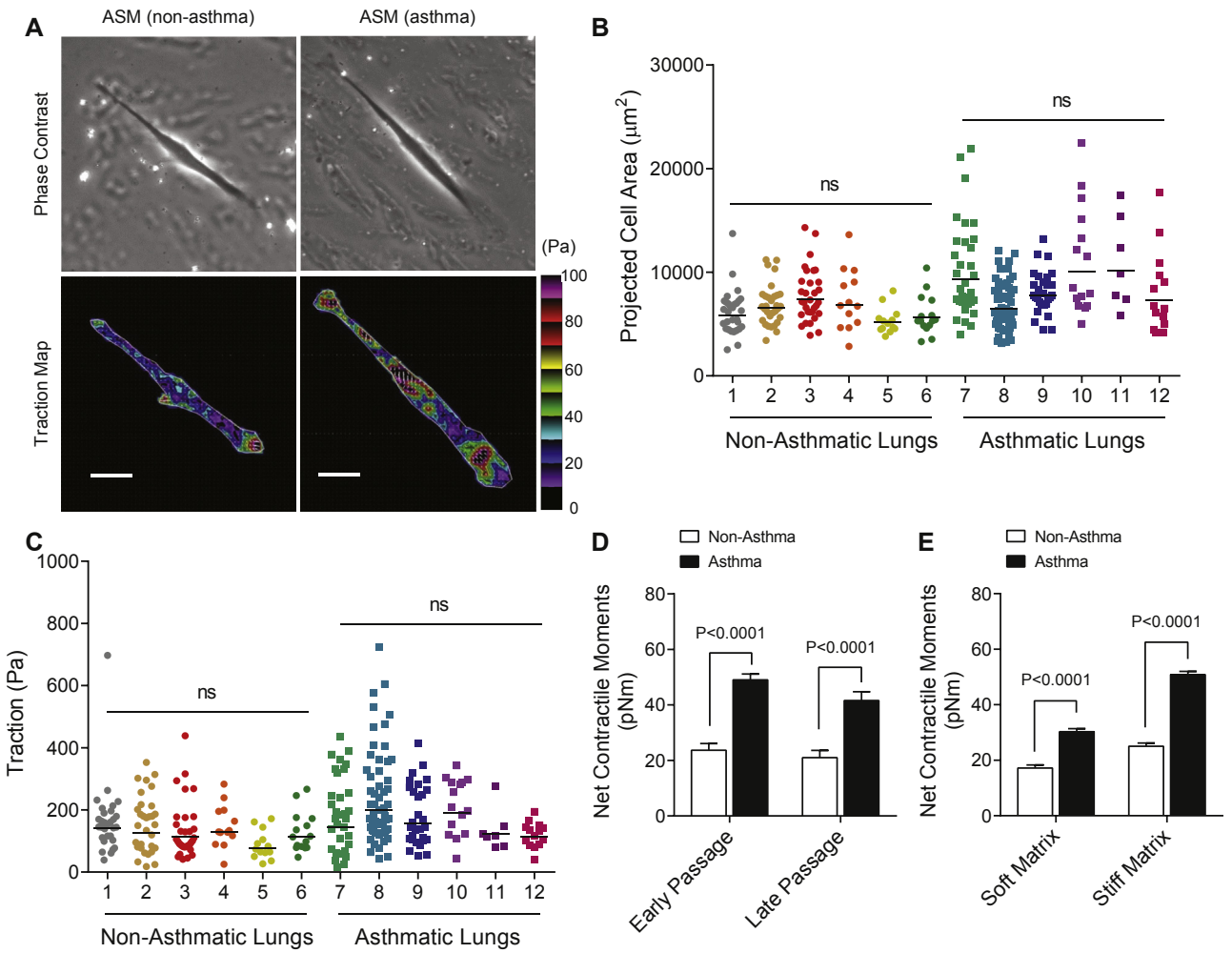

FIG 1. Single-cell analyses on the identity and state of ASM mechanics as measured by Fourier transform traction microscopy. **A,** Representative traction maps of single human ASM cells obtained from donors lungs of those with and without asthma. The *white lines* show the cell boundary, and the colors show the magnitude of the traction in Pascal (Pa) indexed to the *color bar* at the *right*. *Arrows* represent the direction and relative magnitude of the tractions. *Scale bars* represent 50 microns. **B** and **C,** Cell-projected area and traction of isolated human ASM cells (nonasthma, n = 134; asthma, n = 154 individual cell measurements). For these studies, cells were derived from donor lungs of 6 donors without asthma and 6 donors with asthma (Table E1), and plated onto an inert elastic gel (8 kPa) coated with type I collagen. *Bars* are the geometric means of the respective lung donors. **D,** Net contractile moments of human ASM cells in terms of early (passages 1-4: nonasthmatics, n = 69; asthmatics, n = 81) versus late (passages 6-11: nonasthmatics, n = 65; asthmatics, n = 73). **E,** Net contractile moments of human ASM cells measured on the relatively soft (1 kPa: nonasthmatics, n = 43; asthmatics, n = 46) versus the relatively hard (8 kPa: nonasthmatics, n = 34; asthmatics, n = 28) elastic gels. *ns*, Not significant. Data are presented as geometric mean ± SE.

physiologically relevant G protein–coupled receptors, the M_3-muscarinic receptor, and the H_1-histamine receptors, than do ASM cells from those without asthma. We thus conclude that ASM from those with asthma has intrinsic mechanical properties that are hard-wired to the development of airway hyperresponsiveness. These phenotypes are presumably from genetic or epigenetic mechanisms. To date, we have not been successful in ascertaining the distinct polymorphisms or methylation-specific variants that are common across our group of ASM cells derived from subjects with asthma that might account for this mechanical phenotype (data not shown). As might be expected, the number of variants found dictates that a much larger number of ASM samples are needed to infer statistical significance after correcting for multiple comparisons. Last, we have not addressed any additional contribution to ASM phenotypes that arise from airway inflammation, and indeed we contend that asthma susceptibility and exacerbations are dependent on both inflammation-dependent and independent mechanisms.

Tissues for some of our studies were derived from the Gift of Hope Organ & Tissue Donor Network donor families; we thank them for their selfless gift.

Steven S. An, PhD[a,b]
Wayne Mitzner, PhD[a]
Wan-Yee Tang, PhD[a]
Kwangmi Ahn, PhD[c]
A-Rum Yoon, PhD[a]
Jessie Huang, BS[a]
Onur Kilic, PhD[a]
Hwan Mee Yong, MS[a]

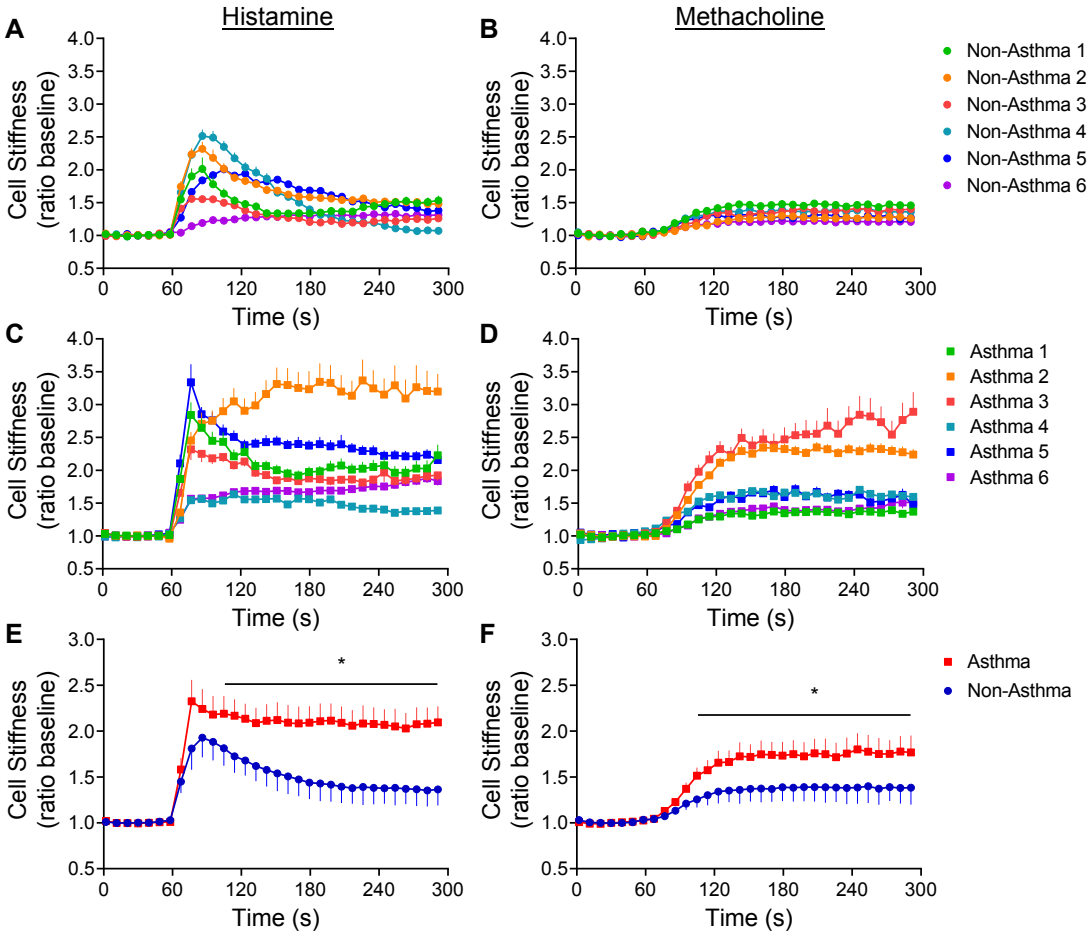

FIG 2. Asthmatic ASM exhibits increased reactivity compared with nonasthmatic ASM as measured by magnetic twisting cytometry. Dynamic changes in cell stiffness in response to 10 μM histamine *(left)* and 10 μM methacholine *(right)* of ASM derived from individual nonasthma (**A** and **B**) and asthma (**C** and **D**) lung donors. Cells were derived from 12 additional donor lungs (Table E2). For each individual human ASM cell, baseline stiffness was measured for the first 60 seconds, and after drug addition stiffness was measured continuously for the next 240 seconds. For each cell, stiffness was normalized to its baseline stiffness before the agonist stimulation. Data are presented as mean ± SE (n = 68-562 individual cell measurements per donor lung). **E** and **F,** Nested model shows increased cell stiffening response to spasmogens in asthmatic ASM compared with nonasthmatic ASM. Data are presented as mean ± SE from donor lungs from 6 donors with asthma and 6 donors without asthma. *$P < .05$.

Jed W. Fahey, PhD[d]
Sarvesh Kumar, PhD[a]
Shyam Biswal, PhD[a]
Stephen T. Holgate, MD[e]
Reynold A. Panettieri, Jr, MD[f]
Julian Solway, MD[g]
Stephen B. Liggett, MD[h]

From [a]the Department of Environmental Health Sciences, The Johns Hopkins University, Bloomberg School of Public Health, Baltimore, Md; [b]the Department of Chemical and Biomolecular Engineering, The Johns Hopkins University, Baltimore, Md; [c]National Institutes of Health, Bethesda, Md; [d]the Department of Pharmacology and Molecular Sciences, Cullman Chemoprotection Center, The Johns Hopkins University, School of Medicine, Baltimore, Md; [e]the School of Medicine, University of Southampton, Southampton, United Kingdom; [f]the Division of Pulmonary, Allergy and Critical Care, Airways Biology Initiative, University of Pennsylvania Medical Center, Philadelphia, Pa; [g]the Department of Medicine, University of Chicago, Chicago, Ill; and [h]the Department of Internal Medicine and Molecular Pharmacology and Physiology, and the Center for Personalized Medicine and Genomics, University of South Florida Morsani College of Medicine, Tampa, Fla. E-mail: san3@jhu.edu. Or: sliggett@health.usf.edu.

This work was supported by the US National Heart, Lung, and Blood Institute (grant nos. HL107361 to S.S.A.; HL114471 to S.S.A., S.B.L., and R.A.P.; and HL097805 to J.S.; and HL45967 to S.B.L.). S.S.A. was also supported by the American Asthma Foundation (Sandler: 108183) grant.

Disclosure of potential conflict of interest: S. S. An, R. A. Panettieri, and S. B. Liggett receive research funding from the National Institutes of Health. J. Solway reports grants from the National Heart, Lung, and Blood Institute during the conduct of the study; personal fees from PulmOne Advanced Medical Devices, Ltd, Israel; personal fees from Hollister, Inc, Wheeling, Ill; personal fees from Cytokinetics, Inc, South San Francisco, Calif; grants from the National Institutes of Health; and grants from AstraZeneca, Inc, outside the submitted work. In addition, J. Solway has patents issued (US Patents #6,090,618, #6,114,311, #6,284,743, #6,291,211, #6,297,221, #6,331,527, and #7,169,764) and a patent PCT/US2014/032186 pending. The rest of the authors declare that they have no relevant conflicts of interest.

REFERENCES

1. de Jongste JC, Mons H, Bonta IL, Kerrebijin KF. In vitro responses of airways from an asthmatic patient. Eur J Respir Dis 1987;71:23-9.
2. Bai TR. Abnormalities in airway smooth muscle in fatal asthma. Am Rev Respir Dis 1990;141:552-7.
3. Bjorck T, Gustafsson LE, Dahlen SE. Isolated bronchi from asthmatics are hyperresponsive to adenosine, which apparently acts indirectly by liberating of leukotrienes and histamine. Am Rev Respir Dis 1992;145:1087-91.

4. Chin LY, Bossé Y, Pascoe C, Hackett TL, Seow CY, Paré PD. Mechanical properties of asthmatic airway smooth muscle. Eur Respir J 2012; 40:45-54.
5. Ijpma G, Kachmar L, Matusovsky OS, Bates JH, Benedetti A, Martin JG, et al. Human trachealis and main bronchi smooth muscle are normoresponsive in asthma. Am J Respir Crit Care Med 2015;191:884-93.
6. An SS, Fabry B, Trepat X, Wang N, Fredberg JJ. Do biophysical properties of the airway smooth muscle in culture predict airway hyperresponsiveness? Am J Respir Cell Mol Biol 2006;35:55-64.
7. Deshpande DA, Wang WC, Mcllmoyle EL, Robinett KS, Schillinger RM, An SS, et al. Bitter taste receptors on airway smooth muscle bronchodilate by localized calcium signaling and reverse obstruction. Nat Med 2010;16: 1299-304.
8. Krzywinski M, Altman N, Blainey P. Points of significance: nested designs. Nat Methods 2014;11:977-8.
9. Salter HH. Asthma: its pathology and treatment, 2nd ed. London: Churchill; 1868.

Available online February 28, 2016.
http://dx.doi.org/10.1016/j.jaci.2015.12.1315

Chronic mucocutaneous candidiasis associated with an SH2 domain gain-of-function mutation that enhances STAT1 phosphorylation

To the Editor:

Signal transducer and activator of transcription 1 (STAT1) transmits signals from interferon receptors and IL-27R.[1] Receptor occupancy results in STAT1 phosphorylation at residue Y701 by receptor-associated Janus kinases (JAKs). STAT1 is recruited to the phosphorylated receptor and gets phosphorylated by receptor-associated JAKs. Phosphorylated STAT1 (pSTAT1) dissociates from the interferon receptor-JAK complex, dimerizes, and translocates to the nucleus where it drives gene transcription.[2] Loss-of-function mutations in STAT1 are associated with intracellular bacterial and viral infections, whereas gain-of-function (GOF) mutations result mainly in chronic mucocutaneous candidiasis with autoimmunity, viral infections, and delayed shedding of deciduous teeth.[3-6] GOF mutations have been identified in the coiled-coil domain and DNA-binding domain of STAT1. They result in decreased STAT1 dephosphorylation, leading to increased pSTAT1 levels and STAT1-driven gene expression.[3-5,7] The enhanced response to IFN-α, IFN-γ, and IL-27, which antagonize the development of T_H17 cells, and the shift from STAT3 to STAT1 signaling by the T_H17-promoting cytokines IL-6 and IL-21, result in defective T_H17 cell differentiation, which underlies the increased susceptibility to chronic mucocutaneous candidiasis.[8] GOF mutations in STAT1 result in the dysregulation of numerous STAT3-controlled genes,[9] which may explain the overlap in the clinical phenotypes due to GOF mutations in STAT1, and loss-of-function mutations in STAT3.

The patient is a 25-year-old woman born to unrelated parents. Beginning at age 5 years, she suffered from recurrent oral and axillary candidiasis, which subsequently involved the vaginal and scalp areas, and from recurrent otitis due to *Pseudomonas* and *Staphylococcus*. At age 7 and 12 years, she had herpes zoster treated with oral acyclovir. At age 12 years, she started having recurrent pneumonias, including *Hemophilus influenza* pneumonia, and bronchitis, and later developed bronchiectasis. At age 16 years, she had amenorrhea, osteopenia, and hypothyroidism, prompting thyroid hormone replacement therapy. She had persistence of deciduous teeth, which required extraction at age 17 years. At age 22 years, she had empyema with sputum culture positive for *Pseudomonas*, and required decortication. At age 24 years, she had resection of the lower lobe of the left lung, which was complicated by empyema.

Immunophenotyping was performed at age 9, 18, and 22 years (see Table E1 in this article's Online Repository at www.jacionline.org). $CD3^+$ T-cell numbers were below or in the lower range of normal, with low numbers of $CD4^+$ T cells and normal numbers of $CD8^+$ T cells. The percentages of naive and memory $CD4^+$ and $CD8^+$ T cells were normal at age 22 years. B-cell numbers progressively decreased from normal to very low, and at age 18 years, her B cells were mostly naive. Natural killer cells decreased from normal to low, but their function was normal (data not shown). Serum IgG, IgA, and IgM off immunoglobulin replacement therapy fluctuated between low and normal. IgE level was not elevated (data not shown). The antibody response to tetanus toxoid was normal (0.52 IU/mL postvaccination; normal, 0.15-7 IU/mL). Protective antibody titers were detected against 7 of 14 serotypes after Pneumovax vaccination. T-cell proliferation at age 22 years was normal to mitogen stimulation, but absent to antigen stimulation.

Whole-exome sequencing revealed a *de novo* heterozygous mutation in exon 22 of *STAT1* (c.1885C>T) in the patient, which was confirmed by Sanger sequencing, and was absent in the parents (Fig 1, *A*, and data not shown). The mutation led to the conversion of a highly conserved histidine at position 629 to tyrosine (p.H629Y) in the SH2 domain of STAT1 (Fig 1, *B*). The mutation was predicted to be benign (score of 0.238) by PolyPhen-2 and tolerated (score of 1.00) by SIFT. Because the features of the patient's phenotype were shared with patients with reported STAT1 GOF mutations (see Table E2 in this article's Online Repository at www.jacionline.org for a comprehensive comparison with other patients with GOF mutations in STAT1), we examined whether her mutation acts as a GOF mutation. Stimulation of EBV-transformed B cells with IFN-γ resulted in increased STAT1 tyrosine phosphorylation in the patient compared with control, as determined by flow cytometry (Fig 1, *C*, left panel) and immunoblotting (Fig 1, *D*) using an anti-pY701 STAT1 antibody. Furthermore, there was increased pSTAT1 nuclear translocation in the patient compared with control (Fig 1, *D*). STAT1 levels were comparable in patient and control (Fig 1, *D*). Stimulation of EBV-B cells with IFN-α also resulted in increased STAT1 tyrosine phosphorylation in the patient compared with control (Fig 1, *C*, right panel). In contrast to normal PBMCs, the patient's PBMCs secreted no detectable IL-17A, but secreted normal amounts of IL-2, in response to anti-$CD3^+$anti-CD28 mAb stimulation (Fig 1, *E*). EBV-B cells from the patient secreted significantly higher amounts of IFN-γ–induced protein-10 than did control cells after IFN-γ stimulation (Fig 1, *F*). These data demonstrate that the H629Y STAT1 mutation is a GOF mutation.[5]

To understand the mechanism of increased STAT1 phosphorylation, we performed a 10-minute time kinetic study of IFN-γ–stimulated EBV-B cells. pSTAT1 accumulation, assessed by flow cytometry, plateaued 4 minutes poststimulation in patient and control, but the level of mutant pSTAT1 was approximately 3-fold higher in the patient at all time points (Fig 2, *A*). To determine whether increased phosphorylation contributed to the higher level of pSTAT1 in the patient, the phosphatase inhibitor orthovanadate was added 5 minutes before IFN-γ stimulation. Significantly more pSTAT1 accumulated in the patient compared with control, indicating increased STAT1 phosphorylation (Fig 2, *B*). To

METHODS

Materials

Unless otherwise noted, all reagents were obtained from Sigma-Aldrich with the exception of Dulbecco modified Eagle medium-Ham's F-12 (1:1), which was purchased from GIBCO (Grand Island, NY). The synthetic arginine-glycine-aspartic acid (RGD)-containing peptide was purchased from American Peptide Company (Sunnyvale, Calif).

ASM cell culture and characterization

Human ASM cells were prepared from donor lungs unsuitable for transplantation in accordance with the respective institutional review boards at the University of Chicago and the University of Pennsylvania. Because the availability of large numbers of early passage primary ASM cells from donor lungs is a challenge, and because the propagation of cells from distal airways often necessitate greater numbers of passages in culture, here we harvested cells from the proximal airways (first- through third-order bronchi) as described.[E1] Cells were maintained in serum-free media for 24 hours at 37°C in humidified air containing 5% CO_2 before study. These conditions have been optimized for seeding cultured cells on collagen matrix and for assessing their mechanical properties.[E1-E5]

Fourier transform traction microscopy

Briefly, cells were plated sparsely on collagen-coated elastic gel blocks precisely tuned to mimic a (patho)physiological range of airway wall rigidity (Young's modulus from 1 to 8 kPa),[E5] and allowed to adhere and stabilize for 24 hours. The contractile stress arising at the interface between each adherent cell and its substrate was measured with traction microscopy,[E4] and the computed traction field was used to obtain net contractile moment, which is a scalar measure of the cell's contractile amplitude. Net contractile moment is expressed in units of pico-Newton meters.

Magnetic twisting cytometry

Dynamic increases in cell stiffness to bronchoconstrictive agonists were measured as an indicator of the single-cell contraction of isolated human ASM cells as we have previously described.[E1-E3] In brief, RGD-coated ferrimagnetic microbeads (4.5 μm in diameter) bound to the cytoskeleton through cell surface integrin receptors were magnetized horizontally and then twisted in a vertically aligned homogeneous magnetic field that was varying sinusoidally in time. This sinusoidal twisting magnetic field caused both a rotation and a pivoting displacement of the bead: as the bead moves, the cell develops internal stresses, which, in turn, resist bead motions.[E3] Lateral bead displacements in response to the resulting oscillatory torque were detected with a spatial resolution of approximately 5 nm, and the ratio of specific torque to bead displacements was computed and expressed here as the cell stiffness in units of Pascal per nanometer.

Statistical analysis

For cell traction force measurements, we used nested design analysis to control for random effects from repeated measurements of multiple cells in the same subject, and to increase the power.[E6] To satisfy the normal distribution assumptions associated with ANOVA, cell traction data were converted to log scale before analyses. Unless otherwise stated, we used Student *t* test and ANOVA with adjustment for multiple comparisons by applying Bonferroni's methods. All analyses were performed using SAS V.9.2 (SAS Institute Inc, Cary, NC), and 2-sided *P* values of less than .05 were considered significant.

REFERENCES

E1. Deshpande DA, Wang WC, Mcllmoyle EL, Robinett KS, Schillinger RM, An SS, et al. Bitter taste receptors on airway smooth muscle bronchodilate by localized calcium signaling and reverse obstruction. Nat Med 2010;16:1299-304.
E2. An SS, Fabry B, Trepat X, Wang N, Fredberg JJ. Do biophysical properties of the airway smooth muscle in culture predict airway hyperresponsiveness? Am J Respir Cell Mol Biol 2006;35:55-64.
E3. Fabry B, Maksym GN, Butler JP, Glogauer M, Navajas D, Fredberg JJ. Scaling the microrheology of living cells. Phys Rev Lett 2001;87:148102.
E4. Butler JP, Tolic-Norrelykke IM, Fabry B, Fredberg JJ. Traction fields, moments, and strain energy that cells exert on their surroundings. Am J Physiol 2002;282:C595-605.
E5. An SS, Kim J, Ahn K, Trepat X, Drake KJ, Kumar S, et al. Cell stiffness, contractile stress and the role of extracellular matrix. Biochem Biophys Res Commun 2009;382:697-703.
E6. Krzywinski M, Altman N, Blainey P. Points of significance: nested designs. Nat Methods 2014;11:977-8.

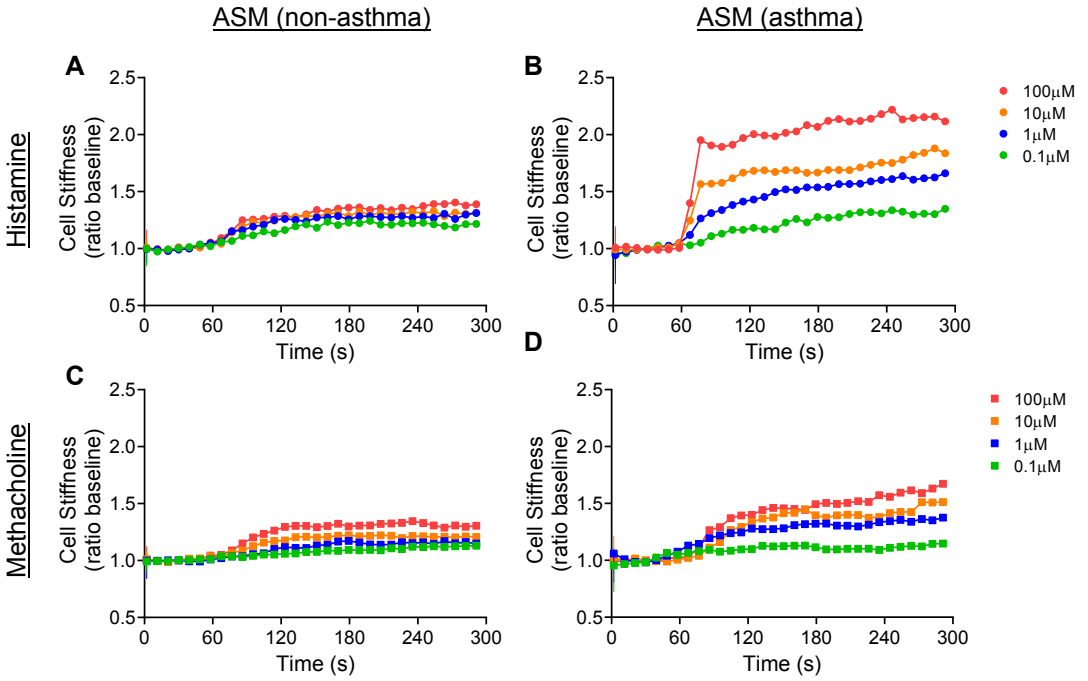

FIG E1. Cell-stiffening responses to histamine (**A** and **B**) and methacholine (**C** and **D**) of ASM derived from lungs of donors without asthma *(left)* and with asthma *(right)* measured by magnetic twisting cytometry. For each individual ASM cell, baseline stiffness was measured for the first 60 seconds, and after drug addition stiffness was measured continuously for the next 240 seconds. For each cell, stiffness was normalized to its baseline stiffness before the agonist stimulation. Data are presented as mean ± SE (n = 68-283 individual cell measurements for each dose of the agonists).

TABLE E1. Characteristics of donor lungs used for cell traction force measurements

Donor	Age (y)	Sex	Race and ethnicity	Cause of death
Nonasthma				
1	25	Male	Unknown	Multiple trauma, anoxia
2	69	Male	Unknown	Intracranial bleed
3	53	Female	White, not Hispanic	Intracranial bleed
4	40	Male	White, not Hispanic	Drug overdose
5	61	Male	Black, not Hispanic	Intracranial bleed
6	49	Male	White, not Hispanic	Intracranial bleed
Asthma				
7	42	Male	Unknown	Unknown
8	44	Female	Unknown	Asthma attack
9	45	Male	White, not Hispanic	Intracranial bleed
10	48	Female	Black, not Hispanic	Intracranial bleed
11	51	Female	Black, unknown	Intracranial bleed
12	11	Male	White, not Hispanic	Anoxia

Human ASM cells used for cell traction force measurements were obtained from the University of Chicago, through the Gift of Hope Organ and Tissue Donor Network.

TABLE E2. Characteristics of donor lungs used for cell stiffness measurements

Donor	Age (y)	Sex	Race and ethnicity	Cause of death
Nonasthma				
13	16	Female	White, not Hispanic	Head trauma
14	37	Male	Black, not Hispanic	Intracranial bleed
15	19	Male	Black, not Hispanic	Closed head injury
16	19	Female	Black, not Hispanic	Head trauma
17	55	Female	Hispanic	Hypertensive bleed
18	55	Female	White, not Hispanic	Central nervous system tumor
Asthma				
19	13	Male	White, not Hispanic	Asthma attack, anoxia
20	44	Male	Hispanic	Asthma attack, anoxia
21	15	Female	Hispanic	Asthma attack, anoxia
22	25	Female	White, not Hispanic	Anoxia
23	38	Male	White, not Hispanic	Asthma attack, anoxia
24	9	Male	White, not Hispanic	Asthma attack

Human ASM cells used for cell stiffness measurements were obtained from the University of Pennsylvania. Lungs were procured through the National Disease Research Interchange and the International Institute for the Advancement of Medicine.